



Published in final edited form as:

*J Pediatr Surg.* 2016 June ; 51(6): 991–994. doi:10.1016/j.jpedsurg.2016.02.066.

## A novel minimal residual disease model of neuroblastoma in mice

Jeremy R. Jackson<sup>a</sup>, Youngleem Kim<sup>a</sup>, Robert C. Seeger<sup>b</sup>, Eugene S. Kim<sup>a,\*</sup>

<sup>a</sup>Division of Pediatric Surgery, Department of Surgery, Keck School of Medicine, University of Southern California, Los Angeles, CA

<sup>b</sup>Department of Pediatrics, Keck School of Medicine, University of Southern California, Los Angeles, CA

### Abstract

**Introduction:** Patients with high-risk neuroblastoma rarely succumb to their primary tumor but rather from relapsed metastatic disease after surgery. We, therefore, sought to create an in vivo model of minimal residual disease (MRD), which clinically replicates tumor recurrence and metastasis after surgical resection.

**Methods:** Neuroblastoma cell lines CHLA-255, CHLA-136, and SH-SY5Y were used. After establishing orthotopic xenografts, mice were divided into control tumor group (sham operation at 14 days) and tumor resection group (resection at 14 days). Mice were monitored by bioluminescent imaging and sacrificed when institutional criteria for euthanasia were met.

**Results:** In the CHLA-255 and CHLA-136 cell lines, mice experienced significantly longer survival following tumor resection ( $p < 0.007$ ). There was no survival benefit seen in the SH-SY5Y cell line ( $p = 0.29$ ). Bioluminescent imaging demonstrated metastatic disease in 100% of all tumor resection mice and varying rates of metastasis in control mice (4 of 5 CHLA-255, 2 of 4 CHLA-136, and 7 of 7 SH-SY5Y).

**Conclusion:** In this study, we describe a novel neuroblastoma model of MRD in mice. This MRD model serves as an innovative means to test preclinical therapies as well as elucidate mechanisms of metastatic disease in experimental neuroblastoma.

### Keywords

Neuroblastoma; Minimal residual disease; Mouse; Model; Resection

---

Neuroblastoma is a heterogeneous, embryonal malignancy of early childhood that is derived from primitive sympathetic ganglion cells. While this cancer can arise anywhere along the sympathetic nerve chain, the majority of these tumors are adrenal in origin. It is the most common pediatric extracranial solid tumor and represents a disproportionately high 15% of all cancer related deaths in children [1]. Despite 5-year survival rates of greater than 90% for low- and intermediate-risk neuroblastoma groups, the survival rate in children

---

\*Corresponding author at: Division of Pediatric Surgery, Children's Hospital Los Angeles, 4650 Sunset Blvd, MS #100, Los Angeles, CA, 90027, USA. Tel.: +1 323 361 8332; fax: +1 323 361 3534. eugenekim@chla.usc.edu (E.S. Kim).

with high-risk neuroblastoma remains 40%–50% [2,3]. High-risk neuroblastoma is generally defined by patient age older than 12 months, evidence of metastatic disease, tumor MYCN gene amplification, and unfavorable pathologic findings. While nearly 80% of high-risk patients will achieve remission through high-dose chemotherapy, surgery, radiation and stem cell transplantation, the majority of patients will eventually succumb to recurrent metastatic disease. Relapse from the presence of minimal residual disease continues to be the most significant barrier to improving the prognosis of those with high-risk tumors.

In research, there are currently three major preclinical mouse models of neuroblastoma: heterotopic, orthotopic and transgenic models. The heterotopic model typically involves the subcutaneous injection of neuroblastoma cells into the flanks of mice [4]. Although this model is easy to perform, the subcutaneous space is not a clinically relevant site for neuroblastoma, and metastases rarely develop. A frequently used orthotopic model entails the injection of tumor cells directly into the subrenal capsule. Despite being difficult to perform successfully in very young mice and requiring increased technical skill, it better simulates the microenvironment in which these tumors normally grow, and the resulting xenografts produce metastases to clinically relevant sites such as the bone marrow, bone, and liver [5,6]. Transgenic mouse models have also been extensively utilized. The TH-MYCN model, in particular, has an overexpression of the oncogene MYCN targeted to neural crest cells, which leads to spontaneous tumorigenesis in the thoracic cavity and adrenal glands of these mice [6,7]. Variances in tumor latency and challenges in breeding frequency make this model more difficult to utilize. However, current mouse models, while useful in evaluating treatment outcomes in the setting of a primary tumor, have provided little insight into the study of tumor recurrence and metastatic disease.

To this end, we developed a novel neuroblastoma model of minimal residual disease to evaluate the processes involved in tumor relapse and metastatic spread as well as their mechanistic origins. Herein, we investigate in several cell lines of human neuroblastoma the incidence of metastasis, recurrence of tumor, and the overall survival rate after surgical resection of orthotopic xenografts when compared to control mice with primary tumors.

## 1. Material and methods

### 1.1. Cell culture and reagents

Three human luciferase-expressing neuroblastoma cell lines (CHLA-255, CHLA-136, SH-SY5Y) were cultured and utilized. The CHLA-255 cell line is MYCN amplified and derived from the brain metastasis of a patient. The CHLA-136 cell line is a particularly chemoresistant cell line with MYCN amplification and was established from the peripheral blood of a patient after chemotherapy and bone marrow transplantation. The SH-SY5Y cell line is non-MYCN amplified and a subclone of the SK-N-SH cell line, derived from a bone marrow biopsy of a patient with thoracic neuroblastoma. CHLA-255 and CHLA-136 were provided by Dr. Robert Seeger (Children's Hospital Los Angeles) and the SH-SY5Y cell line was a gift of Dr. Darrell Yamashiro (Columbia University). Briefly, cell lines were maintained in Iscove's Modified Dulbecco's Medium [CHLA-255 and CHLA-136] or RPMI-1640 Medium [SH-SY5Y]. All media were supplemented with 10% heat-inactivated FBS. On the day of injection, the cells were trypsinized using Puck's EDTA and centrifuged.

The cells were washed with PBS twice and were twice counted using a hemacytometer. The cells were then resuspended in 100  $\mu$ l PBS per  $1 \times 10^6$  cells and stored on ice.

Neuroblastoma cell lines expressing firefly luciferase were generated using a lentiviral transduction technique using standard protocols and a commercially available vector (pGL2-Control vector, Promega, Madison, WI). In brief,  $5 \times 10^6$  293T cells (ATCC #11,268, Manassas, VA) were seeded on 10 cm cell culture dishes and incubated overnight.  $\text{CaPO}_4$  was used for transfection of the luciferase vector followed by sodium butyrate induction about 17 h later. After 48 h of incubation, viral supernatant was ultracentrifuged, and the subsequent viral pellet was dissolved in PBS and stored in a  $-80^\circ\text{C}$  freezer. Neuroblastoma cells,  $2 \times 10^5$ , were incubated overnight in a 12 well plate. Lentiviral-luciferase was used to transduce the neuroblastoma cells for one to two cycles overnight in an incubator. Luciferase positive clones were identified by bioluminescent imaging and subsequently cultured using standard, cell-line specific tissue culture media.

## 1.2. Animal model

Six to eight week old inbred NOD SCID gamma (NSG) mice were used for all studies. Our NSG mouse colony was originally established from mice purchased from Jackson Laboratory and was housed in pathogen-free conditions. All in vivo experiments were approved by the Institutional Animal Care and Use Committee of Children's Hospital Los Angeles (IACUC protocol #363-14). Each mouse was implanted with  $1 \times 10^6$  NB cells (CHLA-255, n = 10; CHLA-136, n = 8; SH-SY5Y, n = 14) into the left subrenal capsule as previously described [5]. In brief, the left flank of anesthetized NSG mice was prepared in a sterile fashion. A transverse left flank incision was performed and the muscle sharply divided. The left kidney was identified and exteriorized out of the wound, and one million neuroblastoma cells in 0.1 ml of PBS were injected into the kidney. The left kidney was placed back into the retroperitoneal space, and the muscle closed with a single 4-0 Vicryl stitch and the skin closed with a skin clip.

After 14 days, a complete resection of the xenograft was performed in half the mice (tumor resection group), while a sham surgery was performed on the other half (control tumor group). All mice were induced in an anesthetic chamber using 2%–2.5% inhaled isoflurane. The mice were transferred onto a sterile field and their left flank was prepared with betadine. Maintenance anesthesia was delivered through a nose cone with 2% isoflurane. A scalpel was used to reopen the previous left flank incision, and the muscle layer was sharply opened. For the control groups, the muscle layer was then reapproximated using 4-0 Vicryl and the skin was closed using a surgical clip. For the tumor resection mice, the left kidney was identified and any adhesions were bluntly dissected. The left kidney was then externalized and a 4-0 Vicryl free tie was used to ligate its hilum. The kidney was then excised. The muscle layer and skin were then closed in layers. Mice were monitored daily and were sacrificed when they met institutional criteria for euthanasia which included weakness/paralysis, seizures, inability to eat or drink, moribund state and dyspnea.

Mice underwent bioluminescent imaging to monitor tumor growth and metastatic disease (Xenogen IVIS Spectrum System, Caliper Life Sciences). The incidence of metastasis was

determined by the presence of a bioluminescent signal at the site of the femurs, liver and/or brain.

### 1.3. Statistical analysis

Survival data were expressed as mean  $\pm$  SD and were analyzed using the Kaplan–Meier method with significance being determined by log-rank test.  $P < 0.05$  was considered significant.

## 2. Results

### 2.1 Minimal residual disease is found in mice after primary tumor resection

In the CHLA-136 group, from the initial 12 mice, 1 mouse died during the orthotopic tumor implantation secondary to anesthesia complications, and 3 mice subsequently died from hemorrhage during tumor resection. Refinement of techniques was made, and all mice in the CHLA-255 and SH-SY5Y groups survived both the orthotopic tumor cell implantation and the subsequent tumor resection surgical procedures.

During early postresection imaging (postoperative day 2), the CHLA-255 tumor resection group showed evidence of MRD in 4 of 5 mice, and at the time of late imaging prior to sacrifice, showed MRD in 5 of 5 mice (Fig. 1). At necropsy, recurrent tumor growth was found in 1 of 5 of the CHLA-255 tumor resection mice. In the CHLA-136 mice, early and late postresection imaging showed evidence of minimal residual disease in 4 of 4 tumor resection mice (Fig. 1). At sacrifice, 4 of 4 tumor resection mice developed recurrent tumors. In the SH-SY5Y group, on early postresection imaging, 6 of 7 tumor resection mice demonstrated evidence of minimal residual disease, and at the time of late imaging prior to sacrifice, showed MRD in 7 of 7 mice (Fig. 1). At necropsy, despite widely aggressive metastatic disease, there were no recurrent tumors in the tumor resection mice.

### 2.2. Increased survival after tumor resection in two of three cell lines

In the CHLA-255 group, mice that underwent tumor resection had a significantly increased mean survival of  $47.4 \pm 1.3$  days compared to  $33.8 \pm 4.1$  days for the control tumor group ( $p = 0.003$ ) (Fig. 2a). Similarly, in the CHLA-136 group, mice that underwent tumor resection also had a significantly increased mean survival of  $44 \pm 3.2$  days compared to  $36 \pm 2.7$  days for the control tumor group ( $p = 0.007$ ) (Fig. 2b). Interestingly, the SH-SY5Y mice showed no difference in mean survival following tumor resection (tumor resection group  $27.6 \pm 2.8$  days vs.  $29 \pm 1.3$  days control tumor group ( $p = 0.29$ ) (Fig. 2c)).

### 2.3. All mice that undergo tumor resection develop metastatic disease

In the CHLA-255 cohort ( $n = 10$ ), all mice in the tumor resection group (5 of 5) had evidence of metastasis to the brain, femur and/or liver at time of sacrifice, compared to 4 of 5 control tumor mice (Fig. 3). Specifically, all mice in the tumor resection group were found to have metastases to the liver; in the control group, 2 mice had metastases to the liver, 2 mice had normal appearing livers, and 1 mouse liver was too necrotic to determine. In the CHLA-136 group ( $n = 8$ ), 4 of 4 tumor resection mice had evidence of metastasis to liver and/or femurs on the day of sacrifice, whereas only 2 of 4 control mice had metastasis

(Fig. 3). All mice in the CHLA-136 tumor resection group demonstrated metastases to the liver, and in the control tumor group, only 2 mice demonstrated overt liver metastases. In the SH-SY5Y cohort (n = 14), at the time of sacrifice, all 7 of 7 tumor resection mice and 7 of 7 control tumor mice were found to have metastases to the liver on imaging as well as grossly (Fig. 3).

### 3. Discussion

Despite escalating intensity of current therapies, approximately 50% of patients with high-risk neuroblastoma eventually relapse and succumb to metastatic disease [3,8,9]. While preclinical models of neuroblastoma have traditionally focused on the treatment of primary disease, no in vivo model has been described to study tumor recurrence and metastasis after surgical resection. In this study, we describe a novel preclinical model of minimal residual disease for neuroblastoma in mice. This MRD model utilizes the advantages of an orthotopic model of neuroblastoma as a foundation for primary tumor engraftment, followed by early surgical resection. Importantly, this clinically relevant model recapitulates metastatic disease seen in patients with high-risk neuroblastoma following surgical resection with subsequent tumor recurrence at the original tumor site and clinically relevant metastases to the liver, bone and bone marrow.

Recent large-scale clinical studies have demonstrated that gross total resection of neuroblastoma confers a survival benefit in patients with high-risk disease [10,11]. In our model, resection of the primary tumor rendered a significant survival advantage in the CHLA-255 and CHLA-136 groups. We did not, however, observe a survival advantage for the tumor resection group in the SH-SY5Y mice. The lack of difference in survival among the SH-SY5Y control and tumor resection groups likely results from rapidly progressing metastatic disease specific to this cell line causing early and robust establishment of metastasis to the liver leading to marked hepatomegaly, prompt clinical deterioration and morbidity. Using this model, we found that the tumor resection groups demonstrated a highly efficient 100% rate of metastatic disease across all three cell lines. In the control tumor groups, the SH-SY5Y group demonstrated a 100% metastasis rate, whereas the CHLA-255 and CHLA-136 control tumor groups inconsistently demonstrated metastatic disease at the time of sacrifice. This consistent rate of metastatic disease is highly advantageous to study targeted therapies for metastasis. Moreover, this model may also serve as an innovative tool to examine the mechanisms of metastatic disease, specifically in neuroblastoma.

Similar to gross total surgical resection of high-risk neuroblastoma in children, the MRD model utilizes a complete tumor resection which leaves behind a microscopic residual amount of tumor which, at times, will give rise to recurrent tumor growth. In comparing the tumor resection groups from the three cell lines, we observed varying rates of tumor recurrence. This tumor recurrence seen in this model also provides a novel means to test the efficacy of future therapies used prophylactically to prevent tumor relapse as well as treatments aimed specifically to residual disease. Ongoing and future studies will utilize this model to study the efficacy of novel immunotherapies as well as targeted therapies to cancer stem cells in experimental neuroblastoma.

With regards to limitations of our mouse model of minimal residual disease, as with any “model” of cancer, no model can completely and perfectly mimic the human disease. In our search for the most clinically relevant model, our goals were primarily to utilize an orthotopic or near-orthotopic model of neuroblastoma, which recapitulates the human disease with large bulky tumors and which metastasizes to clinically relevant organs. Short of experimenting in patients via clinical trials, xenograft mouse models using human cancer cell lines are the primary means by which researchers test novel therapeutics prior to trialing new drugs in patients. While most preclinical mouse models of cancer are focused on the treatment of primary tumors, either in the subcutaneous space (less relevant model) or in an orthotopic location, there have been few mouse models described and practiced which are focused solely on minimal residual disease and metastatic disease. The most popular and technically facile model to study metastatic disease in mice has been the tail vein injection model [12,13]. This model is one in which the researcher injects millions of cancer cells into the tail vein of a mouse, which then indiscriminately sets up foci of metastatic disease. However, this model demonstrates great variability in metastatic disease development and also develops metastasis in clinically irrelevant sites. In addition, it can often take months to see the development of metastatic disease in this model. Our model of MRD based on the resection of a primary orthotopic tumor demonstrates consistent metastatic disease to clinically relevant organs within a short period of time after tumor resection.

Moreover, there are limitations with regards to the many different types of mouse strains used in cancer research. From fully immunocompetent mice to nude mice (T cell deficient), to NOD-SCID (T and B cell deficient), to NSG mice (T and C cell deficient, NK cell deficient), each mouse strain introduces a new set of immunologic variables that can affect tumor take and development of metastasis. In a recent publication [14], Milsom and colleagues found that different models of mice (SCID, NOD-SCID, and NSG mice) led to differing rates of metastasis in a breast cancer model, thus highlighting the importance of the immune state of the host in the process of metastasis. Being the most immunodeficient mouse, NSG mice were found to have the most aggressive metastatic disease, and it is for similar reasons, we have chosen to use the NSG mouse model as the basis to study metastatic disease.

NSG mice have become the working standard for mouse modeling of cancer in basic science research for two primary reasons. First, it is essential to have consistent and reliable tumor development in the utilized model. In immunocompetent mice, tumors, for the most part, do not develop consistently, and tumor take is poor. Only in immunodeficient mice can reliable, robust xenograft tumor development be assured in order to test novel preclinical therapies. Second, an immunodeficient mouse model is necessary to accurately test novel immunotherapies to avoid confounding immunologic variables. It is only through the use of the most immunodeficient mice can you remove as many immunologic factors that may confound findings when studying a novel immunotherapy. Subsequently, additional layers of immunocompetence may be added and used to validate findings, but it is necessary to start with a “blank slate” mouse model to eliminate confounding immunologic variables.



## 4. Conclusions

In this study, we have described a novel murine model of minimal residual disease for neuroblastoma following surgical resection. Using our model, we were able to demonstrate tumor recurrence and a 100% rate of metastatic disease across three human neuroblastoma cell lines in mice. This MRD model could serve as an instrumental tool in the advancement of research into tumor recurrence and metastatic disease in neuroblastoma.

## References

- [1]. Maris JM, Hogarty MD, Bagatell R, et al. Neuroblastoma. *Lancet* 2007;369:2106–20. 10.1016/S0140-6736(07)60983-0. [PubMed: 17586306]
- [2]. Park JR, Eggert A, Caron H. Neuroblastoma: biology, prognosis, and treatment. *Hematol Oncol Clin North Am* 2010;24:65–86. 10.1016/j.hoc.2009.11.011. [PubMed: 20113896]
- [3]. Maris JM. Recent advances in neuroblastoma. *N Engl J Med* 2010;362:2202–11. 10.1056/NEJMra0804577. [PubMed: 20558371]
- [4]. Siegel MM, Chung HS, Rucker N, et al. In vitro and in vivo preclinical chemotherapy studies of human neuroblastoma. *Cancer Treat Rep* 1980;64.
- [5]. Patterson DM, Shohet JM, Kim ES. Preclinical models of pediatric solid tumors (neuroblastoma) and their use in drug discovery. In: Enna SJ, Williams M, Barret JF, Ferkany JW, Kenakin T, Porsolt RD, editors. *Curr. Protoc. Pharmacol.* Hoboken, NJ, USA: John Wiley & Sons, Inc.; 2011.
- [6]. Teitz T, Stanke JJ, Federico S, et al. Preclinical models for neuroblastoma: establishing a baseline for treatment. *PLoS One* 2011;6:e19133. 10.1371/journal.pone.0019133.
- [7]. Weiss WA, Aldape K, Mohapatra G, et al. Targeted expression of MYCN causes neuroblastoma in transgenic mice. *EMBO J* 1997;16:2985–95. 10.1093/emboj/16.11.2985. [PubMed: 9214616]
- [8]. Weinstein JL, Katzenstein HM, Cohn SL. Advances in the diagnosis and treatment of neuroblastoma. *Oncologist* 2003;8:278–92. 10.1634/theoncologist.8-3-278. [PubMed: 12773750]
- [9]. Goldsby RE, Matthay KK. Neuroblastoma: evolving therapies for a disease with many faces. *Paediatr Drugs* 2004;6:107–22. [PubMed: 15035651]
- [10]. Holmes K, Sarnacki S, Poetschger U, et al. Influence of Surgical Excision on Survival of Patients with High Risk Neuroblastoma: Report from Study 1 of Siop Europe (Siopen). Presented at *Advances in Neuroblastoma Research 2014*, Cologne, Germany; 2014.
- [11]. Von Allmen D, Laquaglia MP, Davidoff A, et al. Influence of Extent of Resection on Survival in High Risk Neuroblastoma Patients: A Report from the COG A3973 Study. Presented at *Advances in Neuroblastoma Research 2014*, Cologne, Germany; 2014.
- [12]. Bogenmann E. A metastatic neuroblastoma model in SCID mice. *Int J Cancer* 1996; 67:379–85. 10.1002/(SICI)1097-0215(19960729)67:3<379::AID-IJC1273.0.CO;2-3. [PubMed: 8707412]
- [13]. Khanna C, Hunter K. Modeling metastasis in vivo. *Carcinogenesis* 2005;26:513–23. 10.1093/carcin/bgh261. [PubMed: 15358632]
- [14]. Milsom CC, Lee CR, Hackl C, et al. Differential post-surgical metastasis and survival in SCID, NOD-SCID and NOD-SCID-IL-2R $\gamma$ (null) mice with parental and subline variants of human breast cancer: implications for host defense mechanisms regulating metastasis. *PLoS One* 2013;8:e71270. 10.1371/journal.pone.0071270.

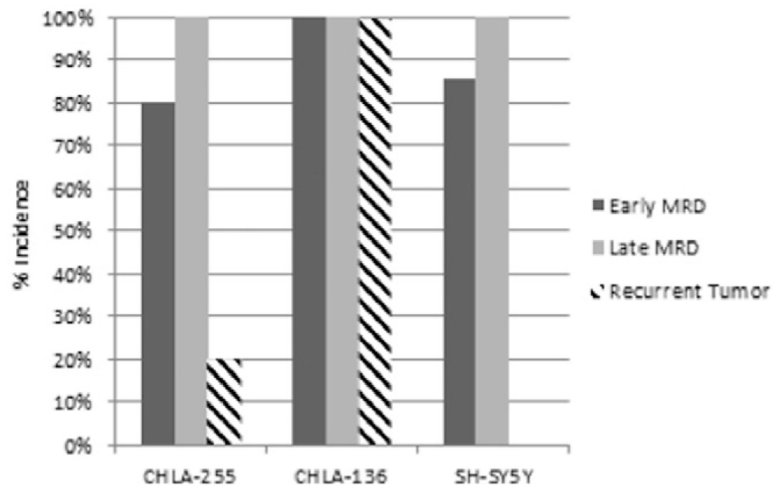


**Fig. 1.** Imaging of the CHLA-255, CHLA-136, and SH-SY5Y mice demonstrated an incidence of minimal residual disease of 80%, 100% and 86%, respectively, at time of first post-resection imaging. All mice demonstrated minimal residual disease at time of sacrifice. At necropsy, tumor recurrence was identified in 20%, 100% and 0% of the CHLA-255, CHLA-136, SH-SY5Y tumor resected mice, respectively.



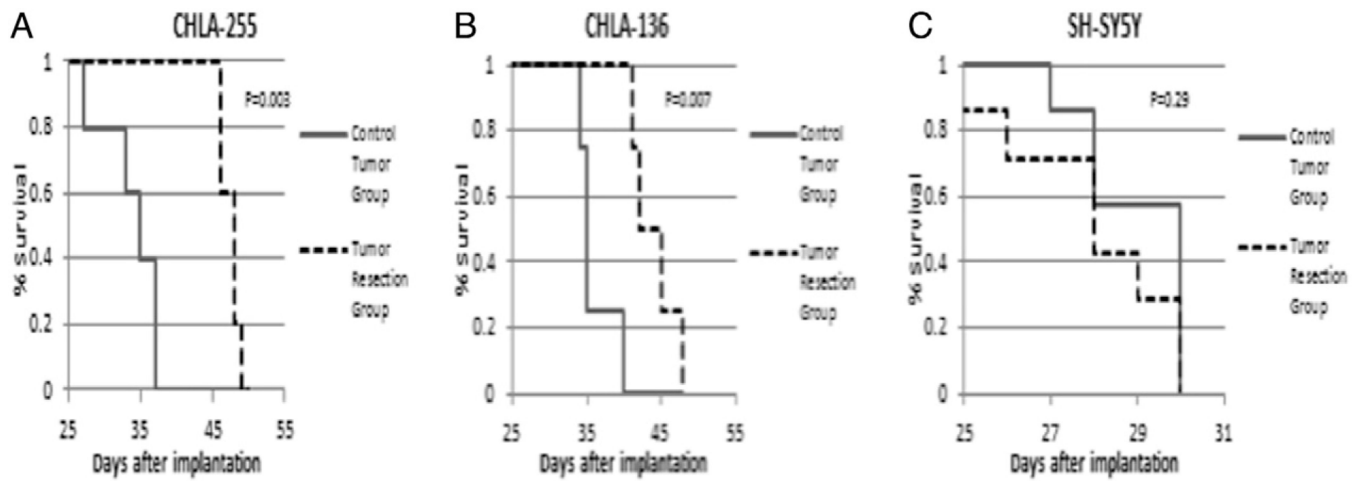


**Fig. 2.**

The CHLA-255 and CHLA-136 tumor resection groups demonstrate significantly increased survival compared to the control groups (CHLA-255 mean survival  $47.4 \pm 1.3$  vs  $33.8 \pm 4.1$  days,  $p = 0.003$ ; CHLA-136 mean survival  $44 \pm 3.2$  vs  $36 \pm 2.7$  days,  $p = 0.007$ ). The SH-SY5Y tumor resection group did not demonstrate a survival benefit (mean survival  $27.6 \pm 2.8$  vs  $29 \pm 1.3$ ,  $p = 0.29$ ).

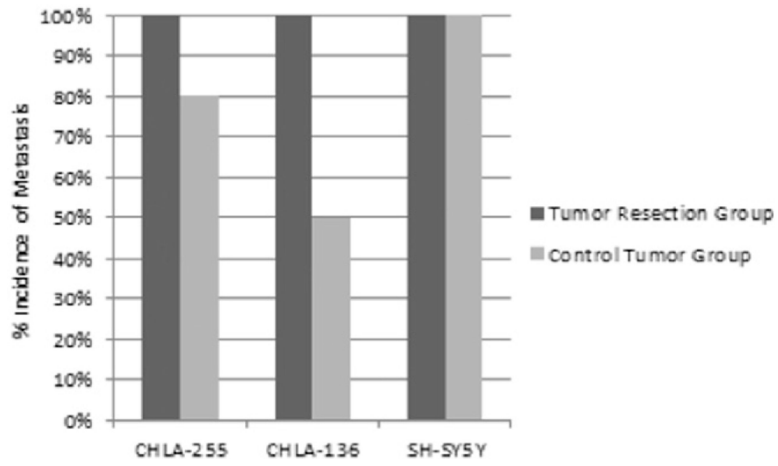


**Fig. 3.** Following tumor resection, 100% of mice demonstrated metastasis on imaging whereas the control tumor groups demonstrated varying rates of metastasis (CHLA-255 80%; CHLA-136 50%; SH-SY5Y 100%).